

Demonstration of High Gain in a Recombination XUV Laser at 18.2 nm Driven by a 20 J, 2 ps Glass Laser

J. Zhang,¹ M. H. Key,^{1,2} P. A. Norreys,² G. J. Tallents,³ A. Behjat,³ C. Danson,² A. Demir,³ L. Dwivedi,³ M. Holden,³ P. B. Holden,⁴ C. L. S. Lewis,⁵ A. G. MacPhee,⁵ D. Neely,² G. J. Pert,⁴ S. A. Ramsden,⁴ S. J. Rose,^{2,6} Y. F. Shao,* O. Thomas,² F. Walsh,² and Y. L. You[†]

¹*Department of Atomic and Laser Physics, University of Oxford, Oxford, OX1 3PU, United Kingdom*

²*Central Laser Facility, Rutherford Appleton Laboratory, Chilton, OX11 0QX, United Kingdom*

³*Department of Physics, University of Essex, Colchester, CO4 3SQ, United Kingdom*

⁴*Department of Physics, University of York, York, YO1 5DD, United Kingdom*

⁵*Department of Pure and Applied Physics, Queen's University, Belfast, BT7 1NN, United Kingdom*

⁶*Department of Physics and Space Science, University of Birmingham, Birmingham, B15 2TT, United Kingdom*

(Received 13 June 1994)

An exceptionally high gain coefficient has been obtained at 18.2 nm in a C VI recombination laser driven by a 2 ps, 20 J, Nd-glass laser operating by chirped pulse amplification. Carbon fiber targets of 7 μm diameter and up to 5 mm length were irradiated at $6 \times 10^{15} \text{ W cm}^{-2}$. The time and space integrated gain coefficient on the 18.2 nm Balmer α transition was measured to be $12.5 \pm 1.5 \text{ cm}^{-1}$. Comparison with numerical modeling suggests that saturated laser action would be obtained with less than a factor of 2 increase in length.

PACS numbers: 42.60.Lh, 32.70.-n, 42.55.Vc, 52.50.Jm

A major objective in the development of extreme ultraviolet (XUV) lasers is to reduce the driver energy significantly below the kilojoule level currently needed for saturated laser action in collisionally excited lasers [1,2]. Adiabatically cooled recombination lasers have long been promising in this respect [3–7] but have so far suffered from a reduction of apparent gain coefficient with increase in plasma length and a consequent limit on the gain-length product to a value much lower than is required to achieve saturated laser action.

One possible solution to this problem is to produce saturated output in a smaller length of plasma by increasing the gain coefficient. We have shown by numerical modeling that this could be achieved for the C VI Balmer α transition at 18.2 nm in less than 1 cm of plasma using a driver laser of picosecond pulse duration, which is much shorter than in earlier work [8]. We report here experimental results of the first observation of high gain in a C VI recombination XUV laser driven by 2 ps, 20 J laser pulses at $\lambda = 1.053 \mu\text{m}$ generated by chirped pulse amplification in a Nd-glass laser [9].

The experimental system had its final compression grating located inside the target chamber under vacuum and an $f/4$ off-axis parabolic mirror reflected the beam to a spot focus which was imaged by an $f/4$ off-axis spherical mirror to produce a line focus 7 mm long and 20 μm wide. The pulse length monitored by a single-shot second-harmonic autocorrelator was 2 ± 0.6 ps. The pulse to background contrast ratio, measured by a single-shot third-order autocorrelation technique, was between 10^6 and 10^7 [9]. The spatially averaged incident irradiance in the line focus was $(6 \pm 1) \times 10^{15} \text{ W cm}^{-2}$ for the data discussed here. There was a fall in focused intensity along the line focus toward the output end

of the plasma due to the geometry and beam intensity profile with an intensity ratio of approximately 1:0.7. About twice the incident energy calculated to be optimum for uniform irradiation was used in the experiment to compensate for the mismatched space-time gain windows with nonuniform irradiation [10].

The targets used in the experiment were carbon fibers of 1 cm length and 7 μm diameter supported at one end. They were positioned with better than $\pm 2 \mu\text{m}$ spatial accuracy and ± 1 mrad angular accuracy using a split-field microscope system [5,7]. The free end of the target was placed well within the line focus to avoid creating a cold output end in the plasma, and the irradiated length was varied by moving the line focus axially along the fiber which was always at the same location.

The primary diagnostic along the fiber axis was a flat-field grazing incidence XUV spectrometer with a 1200 line/mm aperiodically ruled grating. It recorded the spectral range from 5.0 nm to 30.0 nm on Kodak 101-04 film. Spatial resolution in the spectra was provided by two cylindrical mirrors which imaged the fiber end onto the detector plane of the spectrometer giving $\sim 40 \mu\text{m}$ resolution along the direction of the incident laser beam at $2\times$ magnification [11]. Results presented here are effectively spatially integrated, however, as the images produced had a width of the zone of emission no larger than 40 μm . The spectrometer was replaced for some measurements by a normal-incidence concave x-ray multilayer mirror reflecting at 18.2 nm in a bandwidth of 2.0 nm. It was of 250 mm focal length and located 320 mm from the output end of the lasing plasma producing an image at a magnification of $3.6\times$. The detector was an XUV sensitive phosphor coupled to a charged-coupled

device (CCD). A $1.5 \mu\text{m}$ Al filter provided rejection of optical emission.

Off-axis diagnostics included a 2400 line/mm flat-field grating spectrometer at 45° to the fiber axis. It was used to record C v and C vi resonance spectra in the range of 2.0–10.0 nm. The length and uniformity of the plasma were monitored with a x-ray pinhole camera recording an image in emission at wavelengths below 1 nm. A group of Faraday cups gave an estimate of the energy in the plasma and of the angular variation of ion emission.

Two spectra from the on-axis flat-field spectrometer are shown in Fig. 1. The lower spectrum is from a 1 mm irradiated length of carbon fiber at an intensity of $5.6 \times 10^{15} \text{ W cm}^{-2}$. Above it is the spectrum from a 5 mm irradiated length of carbon fiber at a similar intensity of $6.0 \times 10^{15} \text{ W cm}^{-2}$. The C vi Balmer α transition at 18.2 nm and Balmer β transition at 13.5 nm are labeled on the figure. Comparison between the two spectra in Fig. 1 demonstrates a 70 fold enhancement in the on-axis signal for the Balmer α lasing transition as the plasma is lengthened. For measurements at 5 mm length, partial coverage of the detector plane by a $1.6 \mu\text{m}$ thick Al foil filter differentially attenuated (by a factor of 25) the strong Balmer α emission relative to the Balmer β emission in order to allow an accurate measurement of the relative intensity of the two lines. The edge of the filter midway between the Balmer α and β lines could be seen as a step change in intensity of the continuum emission recorded by the spectrometer. The photographic spectra were scanned by a digitizing densitometer, and the resultant density values were converted to the intensity shown in Fig. 1 using calibration data for the response of the film [12]. The intensity of an individual line was obtained by subtracting the background continuum level and integrating spectrally and spatially over the line

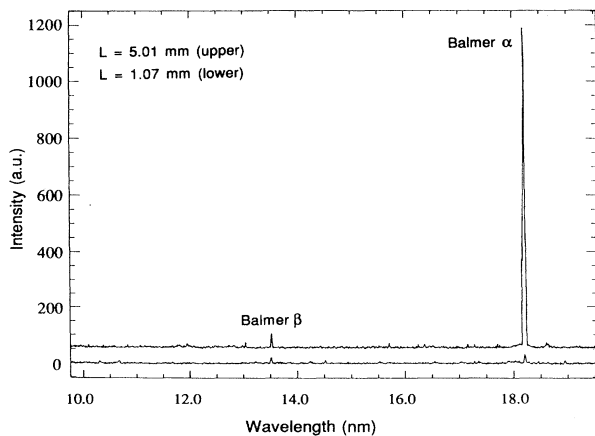


FIG. 1. On-axis spectra for a 1.1 mm long carbon fiber plasma (lower spectrum) and a 5.0 mm long plasma (upper spectrum).

emission. The results of these measurements are plotted in Fig. 2 for the Balmer α and Balmer β lines.

Recombination lasers have a significant amount of fluorescent output from nongain or lower gain zones in space and time. Consequently their apparent gain coefficient, deduced from the space and time integrated increase of intensity with length, should increase with length, becoming asymptotic to the gain in the space-time zone of greatest gain for high gain-length products [13]. The apparent gain coefficient was estimated in this work by least squares fitting of the Linford formula [14] to the data in Fig. 1 giving $12.5 \pm 1.5 \text{ cm}^{-1}$. The procedure underestimates the highest gain which may be present in the best spatial and temporal zone of the plasma. The Balmer β line intensity increased linearly as the plasma length increased, indicating that the line is optically thin.

The ratio of the intensity of the Balmer α transition to that of Balmer β was also determined from each shot. Measurement of this ratio introduces less error due to shot to shot variations than measurements of the intensity of a single line. Figure 3 plots the ratio for different lengths and for comparison shows the predictions of a numerical model [15] for different absorbed laser energies. Modeling and experiment agree best for an absorbed energy of 1.65 J cm^{-1} (about 4% of the laser energy for the 0.5 cm long targets). The apparent gain coefficient in the model deduced in the same way as from the experimental data was 10 cm^{-1} (in reasonable agreement with the value deduced from Fig. 2) while the peak gain coefficient was 19 cm^{-1} .

The absorbed energy was also estimated from measurements of the intensity ratio of resonance lines of C v and C vi [16]. It was inferred to be in the range $0.5\text{--}1.2 \text{ J cm}^{-1}$, and therefore somewhat lower than the estimate from the modeling of the Balmer line ratio.

An image of emission around 18.2 nm from the output end of the lasing plasma is shown in Fig. 4. The image

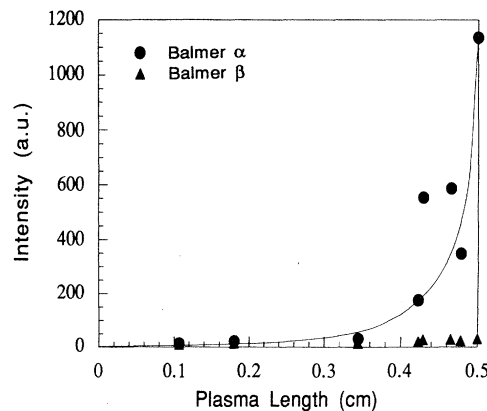


FIG. 2. Intensity of Balmer α and Balmer β lines as a function of the plasma length. Solid dots are data for Balmer α and solid triangles the data for Balmer β .

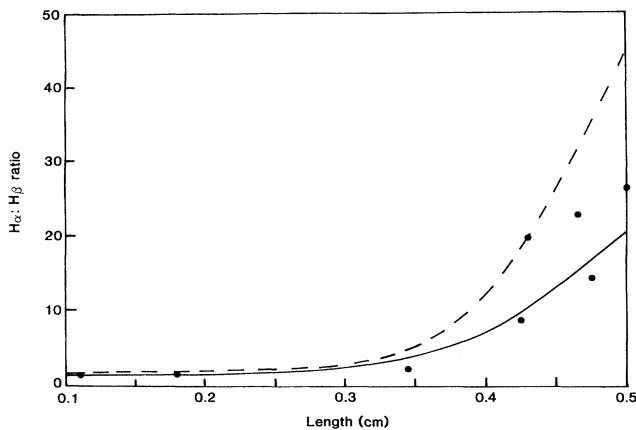


FIG. 3. Intensity ratio of the Balmer α to Balmer β transition measured for different plasma lengths (data points). The curves are computed [15] for different absorbed laser energies (solid line: 1.80 J cm^{-1} ; dashed line: 1.40 J cm^{-1}).

is dominated by Balmer α line emission rather than continuum as the line emission measured in the spectrum shown in Fig. 1 is an order of magnitude stronger than the continuum emission when integrated over a 2.0 nm multilayer mirror bandwidth. The peak intensity region has full widths at half maximum of 20 and $15 \mu\text{m}$ in the horizontal and vertical directions, respectively. The spatial location of the emission peak was estimated to

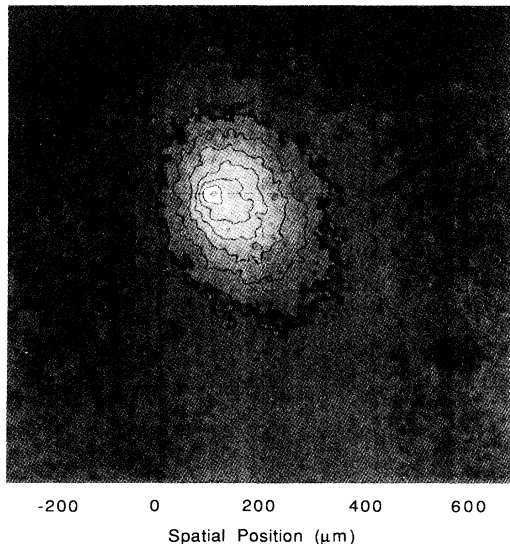


FIG. 4. Image showing the intensity distribution of Balmer α lasing at the exit plane of the recombining plasma. The positions are relative to the initial fiber axis. The plot shows contours representing 3, 5, 9, 14, 28, and 32 relative Balmer α flux density.

be displaced by $100 \pm 50 \mu\text{m}$ toward the laser from the surface of the fiber by comparison with images of continuum emission from a Cu slab target. Modeling [15] predicts that the output intensity should peak at $35 \mu\text{m}$ from the target surface with a spatial image of $10\text{--}15 \mu\text{m}$ (full width at half maximum). This is broadly consistent with the observations within the $\pm 50 \mu\text{m}$ error in the referencing of the spatial location. The effects of beam refraction on the position of the beam in the near field are negligible at the electron densities ($\sim 10^{19} \text{ cm}^{-3}$) where the peak gain exists [8] due to estimated maximum refractive angles of $\leq 1 \text{ mrad}$ (see Ref. [17]).

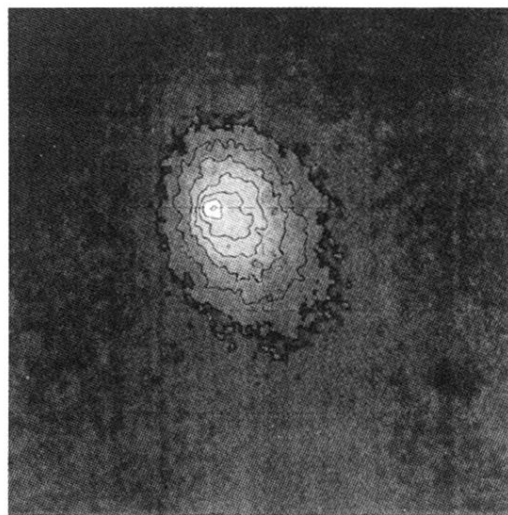
Further evidence that the observed image was that of amplified spontaneous emission (ASE) from the laser was obtained from the agreement of calculated and observed ASE output intensity for a gl product of 6. The calculated intensity was $(2h\nu^3/c^2)(\exp(gl)/\sqrt{gl})\Delta\nu$. The bandwidth $\Delta\nu$ of the ASE was estimated assuming Doppler broadening with a temperature of 10 eV . The experimental intensity was obtained from the CCD image. The sensitivity of the CCD was calibrated to a factor of a few accuracy by comparing its response with Kodak 101 film.

The power density of the source was determined from the data to be $1.4 \times 10^5 \text{ W cm}^{-2}$. It is of interest to compare this with the saturation intensity of the laser predicted by the modeling. The lifetime of the $n = 3$ level was assumed on the basis of modeling to be dominated by Lyman β decay, and the linewidth of the transition was taken to be due to Doppler broadening at 10 eV temperature. The calculated saturation intensity is then calculated to be $2 \times 10^9 \text{ W cm}^{-2}$. The onset of saturation for this laser is predicted using the modeling to occur when the plasma length is about 8 mm . This onset of saturation for a small increase in length reflects the fact that the peak gain is higher than the apparent gain so that with increasing length there should be an increase of apparent gain. A saturated laser of this type would generate a peak power of about 5 kW with a pulse length of about 50 ps and energy of about 200 nJ . The driver energy required would be about 30 J of which only about 1.2 J would be absorbed by the target. The rather low plasma density at the time of laser action implies little refractive distortion relative to collisional lasers so there would be better scope for achieving a diffraction-limited beam.

In conclusion, we have demonstrated that in the C VI recombination XUV laser high gain can be achieved by irradiating fiber targets with ultrashort laser pulses. Our results show the highest gain coefficient observed for the C VI laser. Comparison with modeling suggests that saturated ASE could be produced with a small increase in plasma length.

We would like to thank the VULCAN laser operations, the target preparation, and engineering groups of the Central Laser Facility for their help and cooperation.

- *Scientific visitor from Institute of APCM, Beijing 100088, China.
- †Scientific visitor from Institute of Nuclear Physics and Chemistry, Chengdu 610003, China.
- [1] A. Carillon, H. Z. Chen, P. Dhez, L. Dwivedi, J. Jacoby, P. Jaegle, G. Jamelot, J. Zhang, M. H. Key, A. Kidd, A. Krisnick, R. Kodama, J. Krishnan, C. L. S. Lewis, D. Neely, P. Norreys, D. O'Neill, G. J. Pert, S. A. Ramsden, J. P. Raucourt, G. J. Tallents, and J. Uhmohibhi, *Phys. Rev. Lett.* **68**, 2917 (1992).
- [2] J. A. Koch, B. J. MacGowan, L. B. Da Silva, D. L. Matthews, J. H. Underwood, P. J. Batson, and S. Mrowka, *Phys. Rev. Lett.* **68**, 3291 (1992).
- [3] G. Jamelot, A. Klisnick, A. Carillon, H. Guennou, A. Sureau, and P. Jaegle, *J. Phys. B* **18**, 4647 (1985).
- [4] S. Suckewer, C. H. Skinner, H. Milchberg, C. Keane, and D. Voorhees, *Phys. Rev. Lett.* **55**, 1753 (1985); S. Suckewer, C. H. Skinner, D. Kim, E. Valeo, D. Voorhees, and A. Wouters, *Phys. Rev. Lett.* **57**, 1004 (1986).
- [5] C. Chenais-Popovics, R. Corbett, C. J. Hooker, M. H. Key, G. P. Kiehn, C. L. S. Lewis, G. J. Pert, C. Regan, S. J. Rose, S. Sadaat, R. Smith, T. Tomie, and O. Willi, *Phys. Rev. Lett.* **59**, 2161 (1987).
- [6] Z. Z. Xu, P. Z. Fan, Z. Q. Zhang, S. S. Chen, L. H. Lin, P. X. Lu, L. Sun, X. F. Wang, J. J. Yu, and A. D. Qian, in *X-Ray Lasers 1990*, edited by G. J. Tallents (IOP, Bristol, 1991), p. 151.
- [7] M. Grande, M. H. Key, G. Kiehn, C. L. S. Lewis, G. J. Pert, S. A. Ramsden, C. Regan, S. J. Rose, R. Smith, T. Tomie, and O. Willi, *Opt. Commun.* **74**, 309 (1990).
- [8] J. Zhang and M. H. Key, *Appl. Phys. B* **58**, 13 (1994).
- [9] C. N. Danson, L. J. Barzanti, Z. Chang, A. E. Damerall, C. B. Edwards, S. Hancock, M. H. R. Hutchinson, M. H. Key, S. Luan, R. R. Mahadeo, I. P. Mercer, P. Norreys, D. A. Pepler, D. A. Rodkiss, I. N. Ross, M. A. Smith, R. A. Smith, P. Taday, W. T. Toner, K. W. M. Wigmore, T. B. Winstone, R. W. W. Wyatt, and F. Zhou, *Opt. Commun.* **103**, 392 (1993).
- [10] M. H. Key, S. J. Rose, N. Tragin, and J. Zhang, *Opt. Commun.* **98**, 95 (1993).
- [11] P. Z. Fan, Z. Q. Zhang, J. Z. Zhou, R. S. Jin, Z. Z. Xu, and X. Guo, *Appl. Opt.* **31**, 6720 (1992).
- [12] J. Krishnan, D. Neely, C. Danson, L. Dwivedi, C. L. S. Lewis, and G. J. Tallents, in *Rutherford Appleton Laboratory Annual Report No. RAL-92-020*, 1992 (unpublished), p. 22.
- [13] M. H. Key, N. Tragin, and S. J. Rose, in *X-Ray Lasers 1990*, edited by G. J. Tallents (IOP, Bristol, 1992), p. 163.
- [14] G. J. Linford, E. R. Peressini, W. R. Sooy, and M. L. Spaeth, *Appl. Opt.* **13**, 379 (1974).
- [15] A. V. Borovskiy, P. B. Holden, M. T. M. Lightbody, and G. J. Pert, *J. Phys. B* **25**, 4991 (1992).
- [16] J. Zhang, M. H. Key, P. Norreys, and G. J. Tallents, *Opt. Commun.* **95**, 51 (1993).
- [17] R. C. Elton, *X-ray Lasers* (Academic, New York, 1990), p. 50.



-200 0 200 400 600
Spatial Position (μm)

FIG. 4. Image showing the intensity distribution of Balmer α lasing at the exit plane of the recombining plasma. The positions are relative to the initial fiber axis. The plot shows contours representing 3, 5, 9, 14, 28, and 32 relative Balmer α flux density.